EUROPHYSICS LETTERS 1 December 1996

Europhys. Lett., **36** (7), pp. 483-489 (1996)

Quantum manifestations of chaotic scattering in the presence of KAM tori

M. Eichengrün[1], W. Schirmacher[1] and W. Breymann[2]

[1] *Physik-Department E13, Technische Universität München D-85747 Garching, Germany*

[2] *Institut für Physik, Universität Basel Klingelbergstrasse 82, CH-4056 Basel, Switzerland*

(received 5 July 1996; accepted in final form 23 October 1996)

PACS. 03.65Sq – Quantum mechanics: Semiclassical theories and applications.
PACS. 05.45+b – Theory and models of chaotic systems.
PACS. 72.20−i – Conductivity phenomena in semiconductors and insulators.

Abstract. – We investigate the semiclassical scattering amplitude for systems, where the classical dynamics is non-hyperbolic, *i.e.* where islands of KAM trajectories exist in an otherwise chaotic phase space. With the help of semiclassical calculations for the three-disk billiard in an external magnetic field, in which a hyperbolic–non-hyperbolic transition is observed as a function of the field strength, we show that the "stickiness" of the KAM tori leads to a much slower decrease of the survival probability, as compared with the hyperbolic case. This is reflected by a much narrower shape of the energy correlation function. However, we also find that the algebraic asymptotic decay of the survival probability in the non-hyperbolic case is not important for the quantum fluctuations.

What is the impact of classical chaos on the quantum fluctuations of electrical conductivity? This is an intriguing question, which can be addressed in the framework of the semiclassical description of chaotic scattering. Indeed, quantum fluctuations have recently been shown to reflect some features characterizing classically chaotic dynamics. An example is the classical probability $P_{II'}(E,t)$ of a transition from state I to state I' to occur during the time interval $[t, t+\mathrm{d}t]$. In a pioneering paper Blümel and Smilansky [1] related the energy-dependent autocorrelation function of an S-matrix element, $C_{II'}(\epsilon)$ to the temporal Fourier transform of this probability. The escape of the particles from the scattering region is governed by the phase space structure responsible for the chaotic behavior, namely, the invariant set in form of a chaotic saddle. For hyperbolic systems $P_{II'}(E,t)$ decays exponentially, and therefore the square of the absolute value of $C_{II'}(\epsilon)$ exhibits a Lorentzian peak around $\epsilon = 0$.

The probability $P_{II'}(E,t)$ is directly related to the *survival probability* $N_{II'}(E,t)$, which is the fraction of trajectories $I \to I'$ still in the scattering region at time delay t. Actually $N_{II'}(E,t)$ can be considered as a probability measure, and $P_{II'}(E,t)$ is the corresponding density related to $N_{II'}(E,t)$ by $P_{II'}(E,t) = -\frac{\mathrm{d}}{\mathrm{d}t}N_{II'}(E,t)$. There is strong evidence [2]-[6] that in the presence of stable islands (KAM tori) in an otherwise chaotic phase space, $N_{II'}(E,t)$ exhibits an algebraic asymptotic decay ([1]): $N_{II'}(E,t) \propto t^{-\beta}$. Then, $P_{II'}(E,t)$ asymptotically

([1]) Note that chaotic systems without KAM tori may also exhibit an algebraic asymptotic decay. For example, in the classical s-wave helium model such an algebraic decay of $N(t)$ is observed with $\beta = 0.82$, see [7].

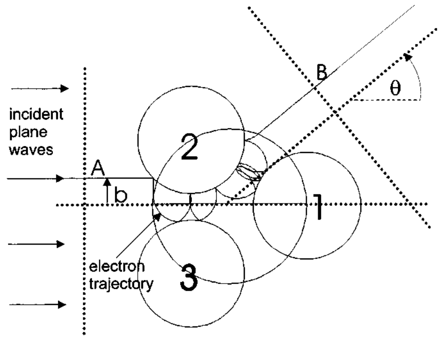

Fig. 1.

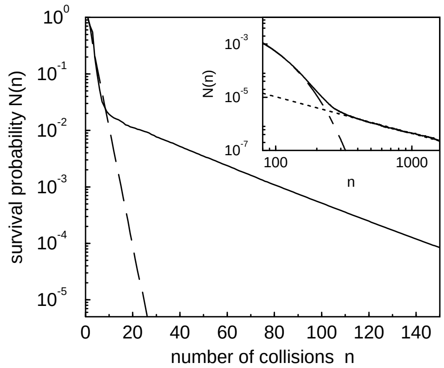

Fig. 2.

Fig. 1. – Scattering geometry for the open three-disk billiard. The classical action (2) is calculated between the points A and B. The disks (radius $r_\mathrm{d} = 1$) are arranged such that their centers form an equilateral triangle (side length $a = 2.5$). The magnetic field $B = \hbar k/qR$ (where R is the cyclotron radius) is assumed to be confined by a circle with radius r_B, which touches the corners of the triangle.

Fig. 2. – Survival probability $N(n)$ *vs.* number of bounces n. Dashed line: $R = \infty$ (hyperbolic case). The slope corresponds to an escape rate $\lambda = 0.48$. Solid line: $R = 0.5$ (non-hyperbolic case). The second slope corresponds to an escape rate $\lambda = 0.038$. Insert: survival probability for large n plotted double-logarithmically. The asymptotic slope corresponds to an exponent $\beta = 1.37$. For comparison the two functions $Cn^{-1.37}$ (dotted) and $\tilde{C}e^{-n0.038}$ (dot-dashed) are shown as well. The calculation for $R = \infty$ was done with initially $5 \cdot 10^6$ trajectories with impact parameters b distributed uniformly in the interval $[-0.75, 0.75]$. The graph for $R = 0.5$ was combined by two calculations, the first with the same initial conditions as for $R = \infty$, the second with $3 \cdot 10^6$ trajectories with impact parameters b distributed uniformly in the interval $[-0.144, -0.14426]$.

decays as $P_{II'}(E,t) \propto t^{-(\beta+1)}$. Correspondingly, at small values of ϵ the energy correlation function should have a contribution $C_{II'}(\epsilon) \propto \epsilon^{\beta}$.

According to numerical studies the exponent β can assume values between 0.5 and 3 [8]; typical values in different models lie around 1.5 [2]-[6]. Note that for values of β larger than 1 there is no initial cusp in $C_{II'}(\epsilon)$. This is in contrast to results reported by Lai *et al.* [9], who concluded that also for $1 < \beta < 2$ the algebraic decay of $N_{II'}(E,t)$ leads to a cusp in $C_{II'}(\epsilon)$ near $\epsilon = 0$ (2).

In addition it is not even clear whether, for non-hyperbolic systems, *observed* correlation functions $C_{II'}(\epsilon)$ will really follow a power law in the $\epsilon \to 0$ limit. Indeed, $N_{II'}(E,t)$ behaves as a power law only after a crossover period. In the case of a scattering experiment where the initial conditions are chosen outside the scattering region this crossover period is much longer (cf. fig. 2) than in the case where the initial conditions are chosen inside the scattering region as in ref. [8]. In any case the non-hyperbolicity leads to a much slower decrease of $N_{II'}(E,t)$ and consequently to a shape of $C_{II'}(\epsilon)$ with a strongly reduced width.

In the following, we shall explicitly show the influence of non-hyperbolicity and the occurrence of stable islands by means of the symmetrical three-disk billiard in a magnetic field. This system, which can be considered as the inner part of a three-lead junction, has been shown [10] to exhibit a hyperbolic–non-hyperbolic transition with increasing field. Here we will concentrate on our main results concerning the survival probabilities and the resulting quantum correlation functions, and we will briefly discuss implications on the universal conductivity fluctuations. A detailed exposition of our calculations will be published in the future [11].

(2) The conclusion in ref. [9] might have been caused by erroneously identifying the survival probability $N_{II'}(E,t)$ with $P_{II'}(E,t)$.

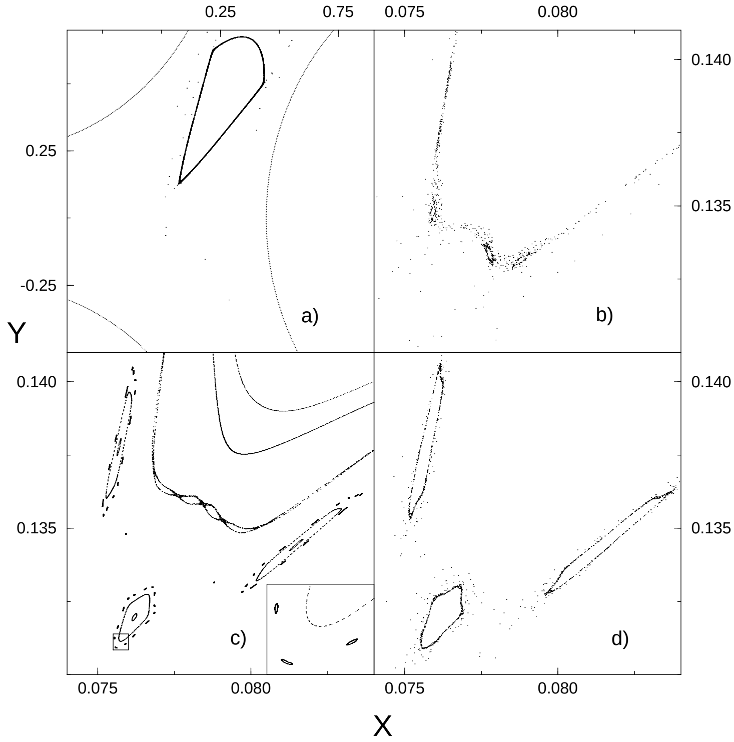

Fig. 3. – *a*) Midpoint coordinates of the cyclotron arcs for two long trajectories with about 3000 bounces. The x and y coordinates of the midpoints of the cyclotron arcs are canonically conjugate to each other, so that the graphs are phase space portraits. *b*), *c*), *d*) Blow-ups of the central part of the phase space; *b*) and *d*) separately display the central parts of the two trajectories; *c*) shows the invariant set in the same region. In the insert the region indicated by the square is magnified again to show the self-similarity. Notice that the scattering trajectories shown in *b*) and *d*) closely follow parts of the islands of the invariant set visible in *c*).

Let us consider electrons in two dimensions (with initial momentum $\mathbf{p} = \hbar k \mathbf{e}_x$) which are scattered from three hard disks in the presence of an external magnetic field characterized by the cyclotron radius $R = \hbar k/eB$ (see fig. 1 for details).

First we study the classical scattering and focus our attention on the fraction $N(n)$ of trajectories which are reflected at least n times (*survival probability*). In fig. 2 we have plotted this function for two qualitatively different cases: i) for $R = \infty$ for which the dynamics is hyperbolic and ii) for $R = 0.5 r_{\mathrm{d}}$, where KAM tori are present. In the hyperbolic regime $N(n)$ decreases exponentially with n, *i.e.* $N(n) \propto \exp[-\lambda n]$, where λ is the escape rate. In the case where the stable trajectories are present, we encounter three regimes in $N(n)$ with qualitatively different behavior: First there is an initial rapid decay ($0 \lesssim n \lesssim 10$) with a slope similar to that of the decay in the hyperbolic regime. In a second regime $10 \lesssim n \lesssim 300$ we find an exponential decay of $N(n)$ with a much smaller decay rate than in the hyperbolic case. It is noteworthy that already in this regime (*i.e.* for $n \gtrsim 25$) the trajectories follow almost exclusively one of the stable orbits. For values of n larger than 300 the decay of $N(n)$ becomes algebraic as can be seen from the insert of fig. 2. In this last regime, which we believe to be the asymptotic one, we have $N(n) \propto n^{-\beta}$ with $\beta = 1.37$. Since the time between two subsequent collisions is almost constant, we have an asymptotic time decay law $N(t) \propto t^{-\beta}$ similar to the behavior reported in other systems with KAM islands.

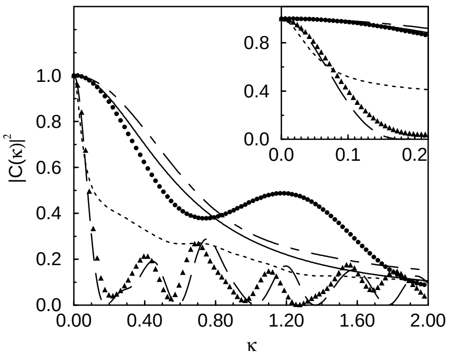

Fig. 4. – Square modulus of the scattering-amplitude autocorrelation function $C_{\theta,R}(\kappa)$ for different cyclotron radii R. Circles: hyperbolic case, $R=\infty$. Triangles: non-hyperbolic case, $R=0.5$. Both calculations were done for $\theta=3.4$, $k_0=1000$, and $\Delta k=1$ (k in units of $1/r_\mathrm{d}$). $f_{k,R}(\theta)$ was calculated by means of eqs. (1) and (2) from initially $2\cdot 10^7$ trajectories with impact parameters b distributed uniformly in the interval $[-0.54, 0.54]$. We also show $|\sum_{n=n_0}^{\infty} P_\theta(n)\exp[i\kappa n\tilde{\delta}]|^2$ (eq. (5)) for $R=\infty$ (full line) and $R=0.5$ (dashed line) with $n_0=4$ and $\tilde{\delta}=0.8$, as well as $|\sum_{n=n_0}^{\infty} P(n)\exp[i\kappa n\tilde{\delta}]|^2$ for $R=\infty$ (dash-dotted line) and $R=0.5$ (dotted line). All curves are normalized to 1 for $\kappa=0$.

To understand why the algebraic decay sets in rather late we take a look at the Poincaré sections of two typical long trajectories (fig. 3) along with the corresponding part of the invariant set. Clearly the trajectories are located at the boundary of a stable island. The invariant set at this boundary exhibits a typical KAM scenario with a self-similar ensemble of stable islands outside the outermost KAM torus. The algebraic decay results from the fact that the long orbits are trapped in the vicinity of this self-similar region which is controlled by a cantor set of destroyed KAM tori (cantorus) [12]. Because of the rather open character of the three-disk billiard (cf. fig. 1) the extent of this region is, however, rather small so that only orbits with more than about 300 reflections experience the self-similarity of the stable islands. Orbits with less reflections follow only the highest member ("state", [12]) of the fractal hierarchy. We conclude that the exponential decay of $N(n)$ in the second time regime is governed by the escape rate from the vicinity of this first state of the hierarchy.

We now turn to the discussion of the quantum scattering amplitude $f_{k,R}(\theta)$. In the semiclassical approximation [13]-[16] $f_{k,R}(\theta)$ takes the familiar form ([3])

$$f_{k,R}(\theta)=\sum_j (c_j(\theta))^{1/2}\exp\left[i\Big[\frac{1}{\hbar}S_j-\frac{\pi}{2}\mu_j\Big]\right]. \tag{1}$$

Here θ is the deflection angle and $c_j(\theta)=\Big|\dfrac{\mathrm{d}\tilde{\theta}}{\mathrm{d}b_j}\Big|^{-1}\Big|_{\tilde{\theta}(b_j)=\theta}$ is the weight of the trajectory j in the classical differential cross-section $\mathrm{d}\sigma/\mathrm{d}\theta$. S_j is the reduced Hamiltonian action along the

([3]) In the presence of the field inside the scattering region the vector potential has to be defined appropriately: $A_r=0$ and $A_\theta=\Phi/(2\pi r)$ for $r\geq r_B$ and $A_\theta=\Phi r/(2\pi {r_b}^2)$ for $r<r_b$, where $\Phi=B\pi r_b^2$ is the magnetic flux. The asymptotic stationary-wave function takes the form $\Psi(x,y)=\Psi(r,\theta)=e^{-i\alpha\theta}e^{ikx}+\frac{f_{k,R}(\theta)}{\sqrt{r}}\,e^{ikr}$, cf. [17].

classical trajectory j from point A_j to B_j (see. fig. 1) defined by

$$S_j = \int_{A_j}^{B_j} \mathbf{p}\mathrm{d}\mathbf{q} - \hbar\alpha\left[(\varphi_{A_j} - \pi) - (\theta - \varphi_{B_j})\right] , \tag{2}$$

where $\alpha = k/2Rr_B^2$. φ_{A_j} and φ_{B_j} are the angular coordinates of the points A_j and B_j and μ is the Maslov index.

In order to study the fluctuations of $f_{k,R}(\theta)$, we define the correlation function

$$C_{\theta,R}(\kappa) = \left\langle \tilde{f}_{k,R}(\theta)^* \tilde{f}_{k+\kappa R}(\theta) \right\rangle_{\Delta k} , \tag{3}$$

where $\langle \ldots \rangle_{\Delta k}$ denotes an average over a range Δk of k values around a central wave number k_0 with $a^{-1} \ll \Delta k \ll k$. The fluctuating part of the scattering amplitude $\tilde{f}_{kR}(\theta)$ is obtained from $f_{kR}(\theta)$ by subtracting off the k average over the range Δk. We now show that $C_{\theta,R}(\kappa)$ is essentially the spatial Fourier transform of the probability density $P(x) = -\frac{\mathrm{d}}{\mathrm{d}x}N(n = x/\delta)$. x is the length of a trajectory and δ is the average path length between two collisions.

Substituting eq. (1) in eq. (3), we get

$$C_{\theta,R}(\kappa) \approx \sum_j c_j(\theta) \exp[i\kappa L_j] , \tag{4}$$

where we have defined effective orbit lengths $L_j := S_j/\hbar k$. In deriving (4) we have neglected the contribution from cross terms because these terms disappear by the average in (3) due to the presence of phase factors with uniformly distributed phases [1]. The sum runs over all trajectories scattered into the angle θ. To evaluate this expression we classify the trajectories by their number n of bounces. This classification takes into account the hierarchical structure of the chaotic invariant set.

The effective length L is approximately proportional to n: $L(n) \approx n\tilde{\delta}$ (4),

$$C_{\theta,R}(\kappa) \approx \sum_n P_\theta(n) \exp[i\kappa n\tilde{\delta}] , \tag{5}$$

where $P_\theta(n) := \sum_j c_j(\theta)\Big|_{n(j)=n}$. The probability $P_\theta(n)\Delta\theta$ is the sum of the lengths of the b-intervals leading to trajectories which make n bounces and are scattered into the angle interval $[\theta, \theta + \Delta\theta]$.

Notice that the outgoing angles of those trajectories which undergo a large number of reflections n are randomly distributed. The reason is the self-similarity of the chaotic invariant set responsible for the chaotic scattering behavior. Thus, in the large-n limit, $P_\theta(n)$ does not depend on θ and is proportional to the integrated probability $P(n) = -\frac{\mathrm{d}}{\mathrm{d}n}N(n)$.

In fig. 4, $|C_{\theta,R}(\kappa)|^2$ calculated by means of (1) and (2) is displayed for the hyperbolic and the non-hyperbolic case (5). In both cases the shape of the correlation function for small κ shows up to be Lorentzian. However, in the non-hyperbolic case the width of this Lorentzian is determined by the small decay rate ($\lambda \simeq 0.038$) of the slow exponential decay of $N(n)$ observed in the intermediate time regime. The results are compared with $|C_{\theta R}(\kappa)|^2$ obtained by means

(4) For $R = \infty$ we have $\tilde{\delta} = \delta$. At finite R there is an extra correction due to the field. We found numerically that for $R = 0.5$ this correction is rather small. In the Fourier transform (5) we took $\tilde{\delta} = 0.8$ for both cases.

(5) The function $C_{\theta,R}(\kappa)$ in fig. 4 was calculated for increasing k_0 and Δk until the results did not change any more.

of eq. (5), *i.e.* the modulus squared of the Fourier transform of $P_\theta(n)$. For comparison, we also show this quantity calculated from $P(n)$ instead of $P_\theta(n)$.

The difference in the behavior of the quantum fluctuations of the scattering amplitudes between the hyperbolic and the non-hyperbolic case is striking (fig. 4): In the hyperbolic case the fluctuations have characteristic wavelengths which are of the same order as the size of the scattering region. In the presence of KAM tori one observes long-wavelength fluctuations which are caused by interference effects due to the trajectories which closely follow the stable orbits. The difference in the fluctuation behavior is also seen very clearly in a direct comparison of scattering amplitudes for the two cases [11].

In the framework of the *diagonal approximation* (4) the correlation function is given as the Fourier transform of $P_\theta(n)$. Thus, the much slower decay of this quantity in the non-hyperbolic case directly causes a much narrower peak of the correlation function. This gives rise to the question up to which $n = n_{\max}$ the function $C_{\theta,R}(\kappa)$ can be determined by the diagonal approximation. The limit $n_{\max}$ can be estimated from the condition that the phase factors in the off-diagonal term should vary rapidly. Thus, for the k values involved in the average (3), one should have $k(L_j - L_\ell) \gg 1$. The smallest occurring length difference ΔL can be estimated to be inversely proportional to the number $A_\theta(n)$ of possible trajectories with n bounces leading into the direction θ: $\Delta L \approx \tilde{\delta}/A_\theta(n)$. For $R = \infty$ we find that $A_\theta(n)$ is represented extremely well by the function $\frac{3}{4}2^n$ owing to the Cantor set structure of the singularities of the function $\theta(b)$ [18]. In the non-hyperbolic case $A_\theta(n)$ increases approximately linearly instead of exponentially and can be approximated by $A(n) \approx -50 + 4.5n$ for $10 \lesssim n \lesssim 40$. For a value of $k_0 = 1000$ we find that in the hyperbolic case $n_{\max} \approx 10$. In the non-hyperbolic case, from extrapolating $A(n)$ we obtain an estimate of $n_{\max} \approx 200$.

In view of these considerations one expects that the algebraic part of $P(n)$ displayed for $n \gtrsim 300$ has hardly any effect on the correlation function. Indeed, on the basis of (5) we only find a very tiny contribution of about 0.1%. Furthermore, the crossover from the slow exponential decay to the asymptotic algebraic decay occurs at values of n for which the diagonal approximation has already broken down. Therefore, in our case, the algebraic decay is irrelevant for the quantum fluctuations. However, this could be different in systems where the algebraic decay sets in earlier.

Finally we want to point out that the same type of analysis also applies for energy-dependent and field-dependent fluctuations of the corresponding correlation functions. Indeed, it can be easily verified that the correlation function $C_{\theta,R}(\kappa)$ is proportional to the energy correlation function $C_\theta(\epsilon)$ with a rescaled energy $\epsilon = 2E\kappa/k$. With this transformation one re-obtains the time-energy Fourier transform of Blümel and Smilansky [1] instead of the space–wave-number transform (5). On the other hand, fluctuations associated with variations of the magnetic field are closely related to the fluctuations of $C_{\theta,R}(\kappa)$ because both k and R enter eq. (2) through the multiplicative term α.

Of course our calculations correspond only to single-channel transmission coefficients, but we believe that the effect will still be visible in the fluctuations of real resistances ([6]). From the above discussion it is obvious that the dimensions of the junctions should not be too small to ensure that the product $k_0 r_{\mathrm{d}}$ is large enough.

We conclude by stating that the presence of KAM tori manifests itself in a striking en-

([6]) We have also started to calculate correlation functions for angle-integrated scattering cross-sections. However, the results differ appreciably from those obtained by applying (5) to the angle-averaged quantities $P_\theta(n)$. The reason is that the latter procedure does not contain interference effects in the correlation function stemming from contributions with different θ. These effects lead to a pronounced peak structure for larger κ. The characteristic range of this structure, again, differs appreciably in the hyperbolic and non-hyperbolic cases.

hancement of the fine-scale quantum fluctuations of the scattering amplitude. This is the consequence of the "stickiness" of the KAM tori. However, we find from our analysis that the algebraic asymptotic decay of the survival fraction $N(t)$ does not have a major influence on these fluctuations. It is rather the very slow exponential decay of $N(t)$ in the intermediate time regime which transforms the structure in the long-wavelength part of the correlation function.

***

The authors are grateful to H. FRIEDRICH and H. THOMAS for illuminating discussions.

REFERENCES

[1] BLÜMEL R. and SMILANSKY U., *Phys. Rev. Lett.*, **60** (1988) 477.
[2] MEISS J. D., CARY J. R., GREBOGI C., CRAWFORD J. D., KAUFMANN A. N. and ABARBANEL H. D., *Physica D*, **6** (1983) 375.
[3] KURNEY C. F. F., *Physica D*, **8** (1983) 360.
[4] CHIRIKOV B. V. and SHEPELYANSKY D. L., *Physica D*, **13** (1984) 395.
[5] MEISS D. and OTT E., *Phys. Rev. Lett.*, **55** (1985) 2741.
[6] DING M., BOUNTIS T. and OTT E., *Phys. Lett. A*, **151** (1990) 395.
[7] HANDKE G., DRAEGER M. and FRIEDRICH H., *Physica A*, **197** (1993) 113; FRIEDRICH H., *Structure and Bonding*, **86** (1996) 97.
[8] LAI Y.-C., DING M., GREBOGI C. and BLÜMEL R., *Phys. Rev. A*, **46** (1992) 4661.
[9] LAI Y., BLÜMEL R., OTT E. and GREBOGI C., *Phys. Rev. Lett.*, **68** (1992) 3491.
[10] BREYMANN W., KOVÁCS Z. and TÉL T., *Phys. Rev. E*, **50** (1994) 1994.
[11] EICHENGRÜN M., SCHIRMACHER W. and BREYMANN W., still unpublished.
[12] See, *e.g.*, MACKAY R. S., MEISS J. D. and PERCIVAL I. C., *Physica D*, **13** (1984) 55; REICHL L. E., *The Transition to Chaos* (Springer-Verlag) 1992, especially pp. 124-148.
[13] JUNG C., *J. Phys. A*, **23** (1989) 1217.
[14] JUNG C. and POTT S., *J. Phys. A*, **23** (1990) 3729.
[15] KNUDSON S. K., DELOS J. B. and BLOOM B., *J. Chem. Phys.*, **83** (1985) 5703.
[16] DELOS J. B., *Adv. Chem. Phys.*, **65** (1986) 161.
[17] PESHKIN M. and TONOMURA A., *The Aharonov-Bohm Effect* (Springer-Verlag, Berlin, Heidelberg, New York) 1989.
[18] ECKHARDT B., *J. Phys. A*, **20** (1987) 5971.